Article

*Discovery Medicine* 2026; 38(207): 1075–1083
https://doi.org/10.24976/Discov.Med.202638207.86

# Protection of N-Butylphthalide in Ischemic Stroke: Ameliorating Neuronal Ferroptosis by Regulating the GSK-3$\beta$/NRF2 Pathway

Yuhuan Cui[1], Youtao Zhang[1], Jiahong Wu[1], Li Zuo[1], Yuanxiang Hu[1], Huihui Liu[1], Shuxian Jia[1], Juan Yan[2], Shutie Li[1,*], Zhankuang Liu[1]

[1]Department of Geriatrics, The First Affiliated Hospital of Hebei North University, 075061 Zhangjiakou, Hebei, China
[2]Department of Pharmacy, The First Affiliated Hospital of Hebei North University, 075061 Zhangjiakou, Hebei, China
*Correspondence: LiSHUTIE_lst@163.com (Shutie Li)
Submitted: 21 January 2026 Revised: 14 February 2026 Accepted: 20 March 2026 Published: 20 April 2026

**Background: N-Butylphthalide (NBP) can effectively improve cerebral vascular microcirculation and cellular energy metabolism in patients with ischemic stroke. This study aims to explore the underlying mechanism by which NBP exerts protective effects in ischemic stroke.**

**Methods: After exposure of primary neuronal cells to different concentrations of NBP (0, 0.1, 1, 10 µM), the optimal concentration for promoting cell survival was determined using a cell counting kit 8 (CCK8) assay. The primary neuronal cell damage model was established with oxygen-glucose deprivation/re-oxygenation (OGD/R), after which treatment with NBP alone or in combination with glycogen synthase kinase 3 beta (GSK-3$\beta$) inhibitors was performed. Cell viability and levels of oxidative stress (lactate dehydrogenase (LDH) and reactive oxygen species (ROS)) were detected. The changes of 4-Hydroxynonenal (4-HNE) and malondialdehyde (MDA) were examined by enzyme-linked immunosorbent assay (ELISA). $Fe^{2+}$ levels, proteins associated with ferroptosis, and the GSK-3$\beta$/nuclear factor erythroid 2-related factor 2 (NRF2) signaling were tested.**

**Results: Both 1 µM and 10 µM NBP effectively alleviated OGD/R-induced cell damage. NBP increased cell viability, inhibited oxidative stress, and down-regulated LDH, ROS, 4-HNE and MDA levels. The cellular $Fe^{2+}$ content was also significantly decreased after NBP treatment. NBP up-regulated ferroptosis-related proteins (glutathione peroxidase 4 (GPX4), solute carrier family 7 member 11 (SLC7A11)) and activated the GSK-3$\beta$/NRF2 signaling. GSK-3$\beta$/NRF2 inhibitors reversed the effects of NBP on OGD/R-induced cells.**

**Conclusion: NBP effectively ameliorates neuronal ferroptosis in ischemic stroke by activating the GSK-3$\beta$/NRF2 signaling pathway, which provides a promising therapeutic strategy and a novel mechanistic basis for clinical management of stroke.**

**Keywords:** N-Butylphthalide; ischemic stroke; ferroptosis; glycogen synthase kinase 3 beta; nuclear factor erythroid 2-related factor 2

## Introduction

The cerebrovascular disease, a kind of central nervous system disorder, has a high incidence at present, with ischemic stroke and hemorrhagic stroke representing the most common clinical forms [1]. Globally, approximately 13.7 million new stroke patients and 5.5 million deaths occur annually, making stroke the second leading cause of mortality [2]. Ischemic stroke, also known as cerebral infarction, constitutes almost 85% of all stroke cases, which is one of the most disabling and lethal diseases among cerebrovascular conditions [3]. Notably, more than 70% of survivors have various degrees of neurological dysfunction [4]. Consequently, developing effective interventions to improve post-stroke neurological dysfunction has become a critical challenge in modern medicine [5].

Clinically, preventing initial or recurrent stroke events is an important therapeutic avenue to reduce neuronal damage and stroke-related mortality [6]. N-Butylphthalide (NBP) is an innovative anti-cerebral ischemia pharmaceutical discovered in China, which has been clinically confirmed to have an efficacy rate of 74.7% in treating ischemic cerebrovascular disorders and a low incidence of adverse reactions [7]. Despite the inadequately defined pharmacological mechanisms of NBP in ischemic stroke, its influence on several pathological processes linked to ischemic cerebral injury and its demonstrated efficacy reflect the promising application of NBP in stroke treatment. Reportedly, NBP can effectively improve cerebral vascular microcirculation and cell energy metabolism in patients with ischemic stroke [8]. Intraperitoneal injection of NBP promotes cytoplasmic-to-nuclear transfer of nuclear factor erythroid 2-related factor 2 (NRF2) protein in a mouse model of traumatic brain injury, thereby suppressing oxidation and alleviating brain injury [9]. NBP can also enhance glycogen synthase kinase 3 beta (GSK-3$\beta$) signaling [10].

Moreover, regulation of GSK-3$\beta$ during ischemic perfusion injury promotes neural stem cell proliferation [11], while GSK-3$\beta$/NRF2 signaling has a neuroprotective effect on ischemic stroke [12]. Multiple studies have found that the activation of NRF2 can alleviate neural stem cell injury in cerebral ischemia-reperfusion injury, highlighting its protective role in ischemic stroke [13,14]. Accordingly, we speculated that NBP may attenuate neuronal ferroptosis through GSK-3$\beta$/NRF2 signaling.

In addition, ferroptosis, as a new type of cell death, is an important mechanism of ischemic stroke. Previous studies have highlighted the significance of NRF2 and ferroptosis in ischemic stroke [15]. NBP has been shown to protect neurons from ferroptosis by activating NRF2 [16]. Based on the above results, we established an oxygen-glucose deprivation/re-oxygenation (OGD/R)-induced cell damage model to investigate whether NBP can suppress neuronal ferroptosis during ischemic stroke by activating GSK-3$\beta$/NRF2 signaling, aiming to provide a theoretical basis for NBP-based ischemic stroke treatment.

## Materials and Methods

### *Cell Culture*

Primary human cortical neuronal cells were obtained from Neuromics (HNC001, Edina, MN, USA), which have been authenticated by short tandem repeat (STR) profiling and tested negative for mycoplasma. These cells were then cultured in neuronal culture medium (HNM0070, Neuromics, Edina, MN, USA) strictly following the culture parameters recommended by Neuromics. Prior to initiating experiments with frozen neurons, primary neurons were passaged two or three times. The cells were cultured in an incubator (Forma Steri-Cult, ThermoFisher, Marietta, OH, USA) at 37 °C with 5% $CO_2$.

### *Establishment and Grouping of OGD/R-Induced Cell Models*

The cells were treated with 0, 0.1, 1 or 10 µM of NBP (HY-B0647, MCE, Monmouth Junction, NJ, USA) for 24 and 72 h, and then two concentrations that promoted cell survival were screened with the cell counting kit 8 (CCK8) assay for follow-up experiments [16]. The cells growing to the logarithmic stage were re-suspended and divided into a control group, an OGD/R group, an OGD/R+NBP-1 group, an OGD/R+NBP-10 group, and an OGD/R+NBP+AR-A014418 group. AR-A014418 is a specific, potent inhibitor of GSK-3$\beta$ with high selectivity over GSK-3$\alpha$ [17]. The OGD/R cell model was established in all experimental groups except the control group, following previously published literature [18]. The cells were cultured in sugar-free DMEM in an anoxic incubator with 94% $N_2$, 5% $CO_2$ and 1% $O_2$ for 6 h, and in a normoxic incubator (reoxygenation) with 5% $CO_2$ at 37 °C for 24 h. Cells in the control group were cultured in complete medium under normoxic conditions throughout the experiment. Then, the cells of the OGD/R+NBP-1 and OGD/R+NBP-10 groups were cultured with NBP at concentrations of 1 µM and 10 µM for 24 h, respectively, and the cells of the OGD/R+NBP+AR-A014418 group were co-treated with NBP (10 µM) and AR-A014418 (5 µM, HY-10512, MCE, USA) for 24 h.

### *CCK8*

The cells in the logarithmic growth phase were seeded into 96-well plates (167008, Thermo Fisher, Waltham, MA, USA) at approximately 5000 cells/well and incubated overnight in a $CO_2$ incubator. After the cells were attached to the wall, they were treated according to the respective experimental group, while cells in the control group were treated with an equivalent volume of double-distilled water. Cells were cultured in 96-well plates for 24 h and 72 h, followed by the addition of 10 µL of CCK8 reagent (C0038, Beyotime, Shanghai, China) and incubation for 2 h. The absorbance at 450 nm was measured using a microplate reader (VLBL00GD2, Varioskan LUX, Thermo Fisher, USA).

### *Lactate Dehydrogenase (LDH) Release Method*

The cells were inoculated into 96-well plates at a density of $2 \times 10^4$ cells/well and received corresponding treatments according to the groups. The supernatant of each group was mixed with 60 µL LDH test solution according to the instructions of the LDH cytotoxicity detection kit (C0016, Beyotime, China), and incubated at ambient temperature for 30 min in the dark. The absorbance was ultimately measured at 490 nm using a microplate reader, and 6 multiple wells were set up in each group.

### *Dichlorodihydrofluorescein Diacetate (DCFH-DA)*

After 24-h culture, cells were digested into a single-cell suspension with pancreatic enzyme (25200056, Gibco, Waltham, MA, USA) and centrifuged in a centrifuge tube at 4 °C for 5 min. The supernatant was discarded, and then 10 µmol/L DCFH-DA working solution (HY-K0320, MCE, USA) diluted with serum-free DMEM was added to each tube and incubated at 37 °C for 20 min. Next, the cells were placed under a fluorescence microscope (100×, THUNDER Imager Tissue, Leica, Wetzlar, Germany) to observe the fluorescence signal, and the relative reactive oxygen species (ROS) content in the cells was calculated using Image-Pro Plus software (version 6.0, Media Cybernetics, Inc., Rockville, MD, USA).

### *Enzyme-Linked Immunosorbent Assay (ELISA)*

Following 24-h culture according to the groups, cells were washed with phosphate buffer saline (PBS; C0221A, Beyotime, China), where levels of 4-Hydroxynonenal (4-HNE) (D751041-0096, Sangon Biotech, Shanghai, China) and malondialdehyde (MDA) (E-EL-0060, Elabscience, Wuhan, China) were determined as per the manual of the

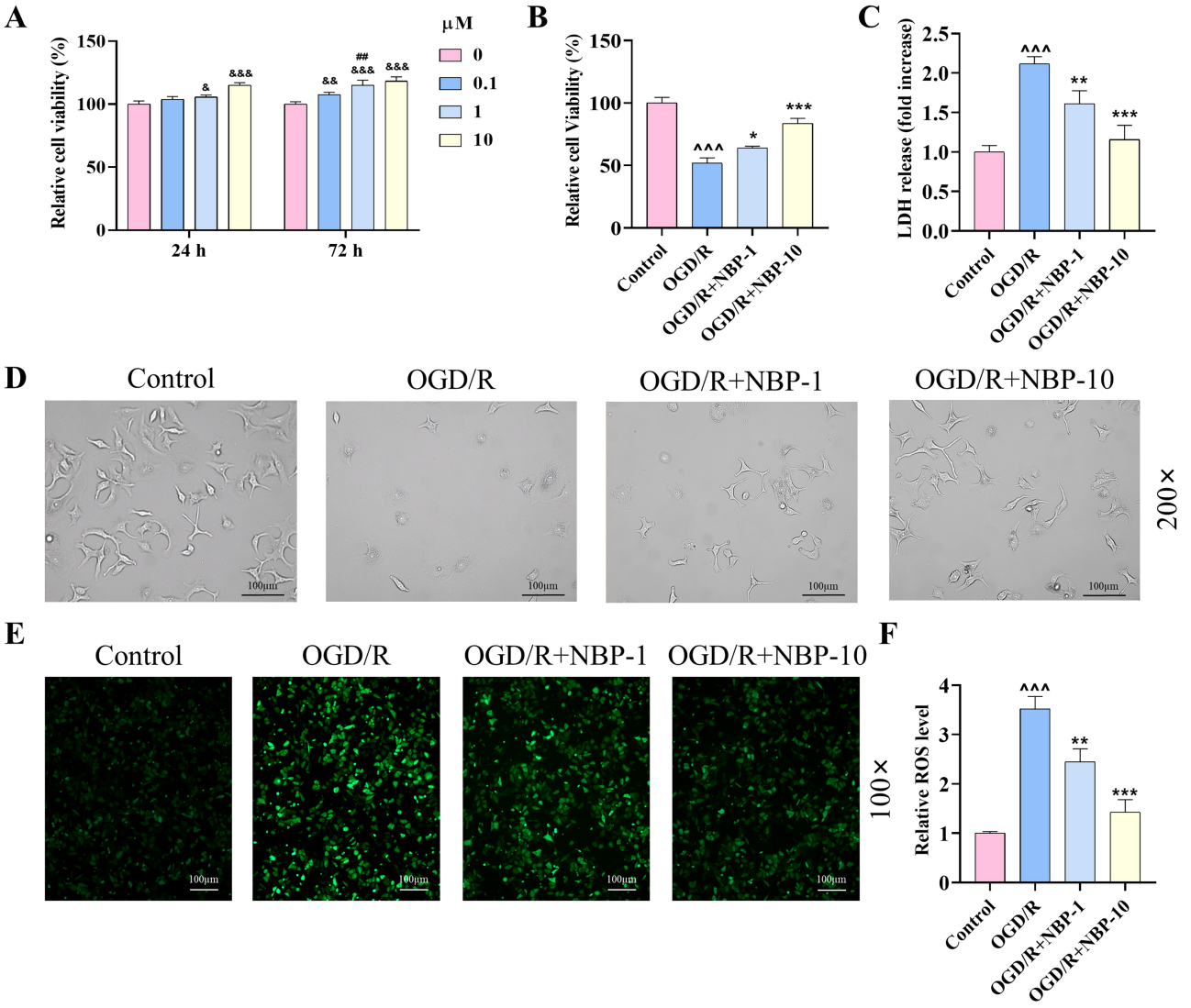


**Fig. 1. N-Butylphthalide (NBP) enhanced neuronal cell viability and reduced lactate dehydrogenase (LDH) and reactive oxygen species (ROS) levels after oxygen-glucose deprivation/re-oxygenation (OGD/R) treatment.** (A) After cells were cultured with different concentrations of NBP (0, 0.1, 1, 10 μM) for 24/72 hours (h), the survival rate of neuronal cells was measured by cell counting kit 8 (CCK8). (B) The OGD/R model of primary neuronal cells was established, and cell viability was examined after treatment with 1 μM and 10 μM NBP. (C) Detection of LDH levels in each group. (D) Morphological observation of cells. Scale: 100 μm, magnification: 200×. (E,F) Dichlorodihydrofluorescein diacetate (DCFH-DA) was used to detect intracellular ROS levels. Scale: 100 μm, magnification: 100×. All datasets were derived from three independently repeated experiments. $^{\&}$vs. 0 μM, $^{\&}p < 0.05$, $^{\&\&}p < 0.01$, $^{\&\&\&}p < 0.001$; $^{\#}$vs. 24 h, $^{\#\#}p < 0.01$; $^{*}$vs. OGD/R, $^{*}p < 0.05$, $^{**}p < 0.01$, $^{***}p < 0.001$; $^{\wedge}$vs. Control, $^{\wedge\wedge\wedge}p < 0.001$.

ELISA kit. Firstly, the cell culture medium was collected and centrifuged at 1000 rpm for 20 min at 4 °C to remove cell debris and impurities. Then, the supernatant was collected, and the corresponding reagents were added according to the manufacturer's instructions. Finally, the absorbance was measured at 450 nm using the microplate reader.

### *Intracellular $Fe^{2+}$ Content Detection*

After indicated treatment in each group, cells were digested in pancreatic enzymes and centrifuged at 1200 rpm for 4 min. After the collection of cell precipitates, $5 \times 10^6$ cells were added with 1 mL of reagent 1, and the cells were broken by ultrasonic wave under an ice bath for 5 min and finally centrifuged at 10,000 g and 4 °C for 10 min. The supernatant was collected and placed on ice until analysis. According to the manufacturer's instructions, the $Fe^{2+}$ content detection kit (BC5415, Solarbio, Beijing, China) was added for reaction, and the absorbance was measured at 593 nm using the microplate reader.

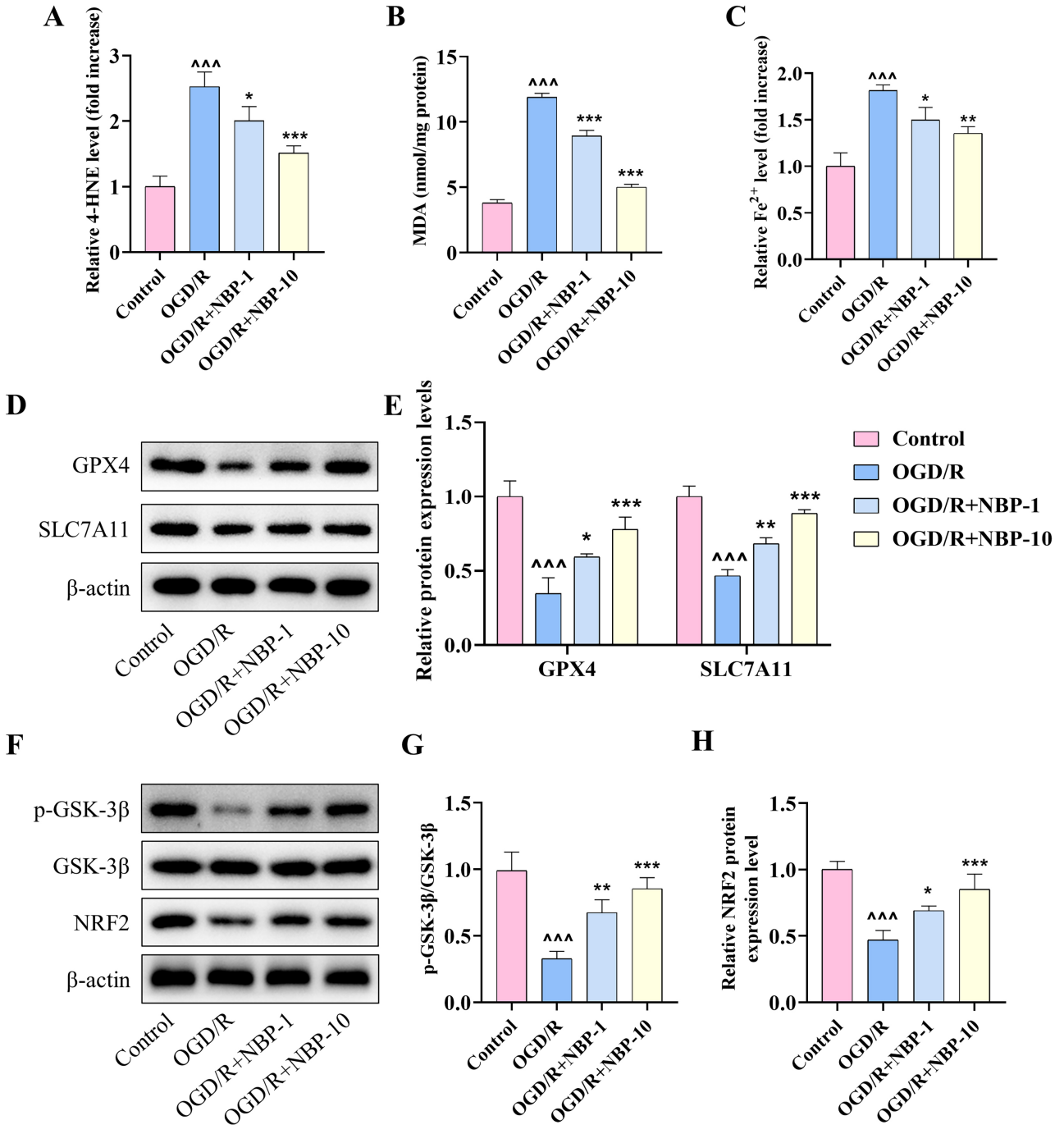


**Fig. 2. NBP abrogated OGD/R-induced ferroptosis via activating GSK-3$\beta$/NRF2 signaling.** (A,B) Enzyme-linked immunosorbent assay (ELISA) was used to detect 4-Hydroxynonenal (4-HNE) and malondialdehyde (MDA) levels. (C) Detection of intracellular $Fe^{2+}$ content. (D,E) Western blot analysis of ferroptosis-related proteins glutathione peroxidase 4 (GPX4, 17 kDa) and solute carrier family 7 member 11 (SLC7A11, 55 kDa). $\beta$-actin (42 kDa) was the internal reference. (F–H) Western blot analysis of glycogen synthase kinase 3 beta (GSK-3$\beta$, 47 kDa) phosphorylation and nuclear factor erythroid 2-related factor 2 (NRF2, 97 kDa) protein levels. $\beta$-actin (42 kDa) was the internal reference. All datasets were derived from three independently repeated experiments. $^{\wedge}$vs. Control, $^{\wedge\wedge\wedge}p < 0.001$; $^{*}$vs. OGD/R, $^{*}p < 0.05$, $^{**}p < 0.01$, $^{***}p < 0.001$.

*Western Blot Analysis*

Total protein was extracted from cells using radioimmunoprecipitation assay (RIPA) lysate (R0010, Solarbio, China). The protein concentration was then quantified with the bicinchoninic acid assay (BCA; P0012, Beyotime, China). The proteins were separated by sodium dodecyl sulfate polyacrylamide gel electrophoresis (SDS-PACE; P0014A, Beyotime, China), and transferred onto a

polyvinylidene fluoride (PVDF) membrane (YA1700, Solarbio, China) using a wet transfer method. The membrane was blocked using 5% skim milk at room temperature for 1.5 h, and incubated firstly with primary antibodies overnight at 4 °C and then with secondary antibodies (ab6721, Abcam, UK, 1:2000; ab6708, Abcam, Cambridge, UK, 1:3000) for 2 h the following day. The gel imaging device (GD50302, Monad, Wuhan, China) was used to expose the strips, and ImageJ software (version 1.50i, National Institutes of Health, Bethesda, MD, USA) was applied to examine the gray values. The primary antibodies included p-GSK-3$\beta$ (ab75745, Abcam, UK, 47 kDa, 1/1000), GSK-3$\beta$ (ab93926, Abcam, UK, 47 kDa, 1/1000), NRF2 (#12721, CST, USA, 97 kDa, 1/1000), glutathione peroxidase 4 (GPX4) (ab125066, Abcam, UK, 17 kDa, 1/1000), solute carrier family 7 member 11 (SLC7A11) (ab307601, Abcam, UK, 55 kDa, 1/1000), and $\beta$-actin (internal reference) (ab8226, Abcam, UK, 42 kDa, 1 µg/mL).

### *Statistical Analysis*

Statistical analysis was conducted utilizing GraphPad Prism 8.0 (GraphPad Software, USA). Measurement data are presented as mean ± standard deviation. One-way analysis of variance (ANOVA) was employed to compare multiple groups. The Sidak test was applied for post-hoc tests. A $p$-value of less than 0.05 was deemed statistically significant.

## Results

### *NBP Enhanced Neuronal Cell Viability and Reduced LDH and ROS Levels After OGD/R Stimulation*

We first screened the optimal NBP concentration to promote primary neuronal cell survival through the CCK8 assay. The experimental results showed that treatment with different concentrations of NBP (0, 0.1, 1, 10 µM) for 24/72 h increased cell viability to varying degrees (Fig. 1A). Notably, NBP (1 and 10 µM) treatment at 24 and 72 h was associated with the most significantly enhanced cell viability (Fig. 1A, $p < 0.05$). Moreover, after treatment with 1 µM NBP, the cell viability at 72 h was higher than that at 24 h (Fig. 1A, $p < 0.01$). We selected 1 and 10 µM concentrations for subsequent experiments due to their consistent pro-survival effects across both 24 h and 72 h, whereas 0.1 µM only showed significant efficacy at 72 h. Subsequently, we constructed the OGD/R-induced cell model and found that both 1 µM and 10 µM NBP markedly increased cell viability after OGD/R treatment (Fig. 1B, $p < 0.05$). In addition, after OGD/R treatment, the cell morphology was abnormal (blurred cell edges), and the levels of LDH and ROS were markedly elevated, with ROS green fluorescence intensity considerably heightened in comparison to the control group (Fig. 1C–F, $p < 0.001$). In contrast, NBP treatment improved the cell morphology and decreased the levels of LDH and ROS (Fig. 1C–F, $p < 0.01$).

### *NBP Abrogated OGD/R-Induced Ferroptosis via Activating GSK-3$\beta$/NRF2 Signaling*

ELISA experiment data revealed that both concentrations of NBP (1, 10 µM) significantly down-regulated 4-HNE and MDA in cells after OGD/R treatment (Fig. 2A,B, $p < 0.05$). Also, OGD/R treatment elevated $Fe^{2+}$ level in primary neuronal cells, which was reversed by NBP (Fig. 2C, $p < 0.05$). To demonstrate the regulation of ferroptosis and GSK-3$\beta$/NRF2 signaling in primary neuronal cells by NBP, we examined the levels of related proteins in cells by Western blot analysis. The results indicated that OGD/R treatment down-regulated the ferroptosis proteins GPX4 and SLC7A11 in primary neuronal cells, and inhibited GSK-3$\beta$/NRF2 signaling, as demonstrated by the down-regulation of p-GSK-3$\beta$/GSK-3$\beta$ and NRF2 proteins (Fig. 2D–H, $p < 0.001$). In contrast, NBP treatment reversed these regulatory effects of OGD/R on ferroptosis and GSK-3$\beta$/NRF2 signaling (Fig. 2D–H, $p < 0.05$). 10 µM NBP was selected for intervention therapy in the follow-up experiment.

### *GSK-3$\beta$/NRF2 Inhibitors Offset the Effects of NBP on Cell Viability, LDH Level and ROS Level*

To further investigate the regulatory mechanism of NBP on ferroptosis in ischemic stroke neurons, we treated the cells with GSK-3$\beta$/NRF2 inhibitors and NBP. In the detection of cell viability, our experiments demonstrated that NBP boosted cell viability in OGD/R-treated cells, which was counteracted by the GSK-3$\beta$/NRF2 inhibitor AR-A014418 (Fig. 3A, $p < 0.01$). Furthermore, AR-A014418 abrogated NBP-induced down-regulation of LDH and ROS in model cells, and elevated their levels (Fig. 3B–D, $p < 0.05$). These results suggested that NBP could alleviate neuronal damage in the ischemic brain by activating GSK-3$\beta$/NRF2 signaling.

### *GSK-3$\beta$/NRF2 Inhibitors Reversed the Effects of NBP on OGD/R-Induced Neuronal Ferroptosis*

ELISA results showed that GSK-3$\beta$/NRF2 inhibitor AR-A014418 reversed the inhibitory effect of NBP treatment on 4-HNE and MDA levels in model cells (Fig. 4A,B, $p < 0.01$). According to the detection results of $Fe^{2+}$ level, we confirmed that NBP treatment significantly suppressed the increase of $Fe^{2+}$ level after OGD/R treatment; however, AR-A014418 treatment neutralized this inhibiting effect of NBP (Fig. 4C, $p < 0.05$). Ferroptosis and GSK-3$\beta$/NRF2 signal-related proteins were quantified in each group. NBP treatment suppressed ferroptosis and activated the GSK-3$\beta$/NRF2 signaling in OGD/R-induced cells, while AR-A014418 reversed this effect of NBP by down-regulating ferroptosis proteins GPX4 and SLC7A11, as well as p-GSK-3$\beta$/GSK-3$\beta$ and NRF2 in GSK-3$\beta$/NRF2 signaling (Fig. 4D–H, $p < 0.05$). The results corroborated that NBP might activate GSK-3$\beta$/NRF2 signaling, which in turn could reduce neuronal ferroptosis caused by OGD/R.

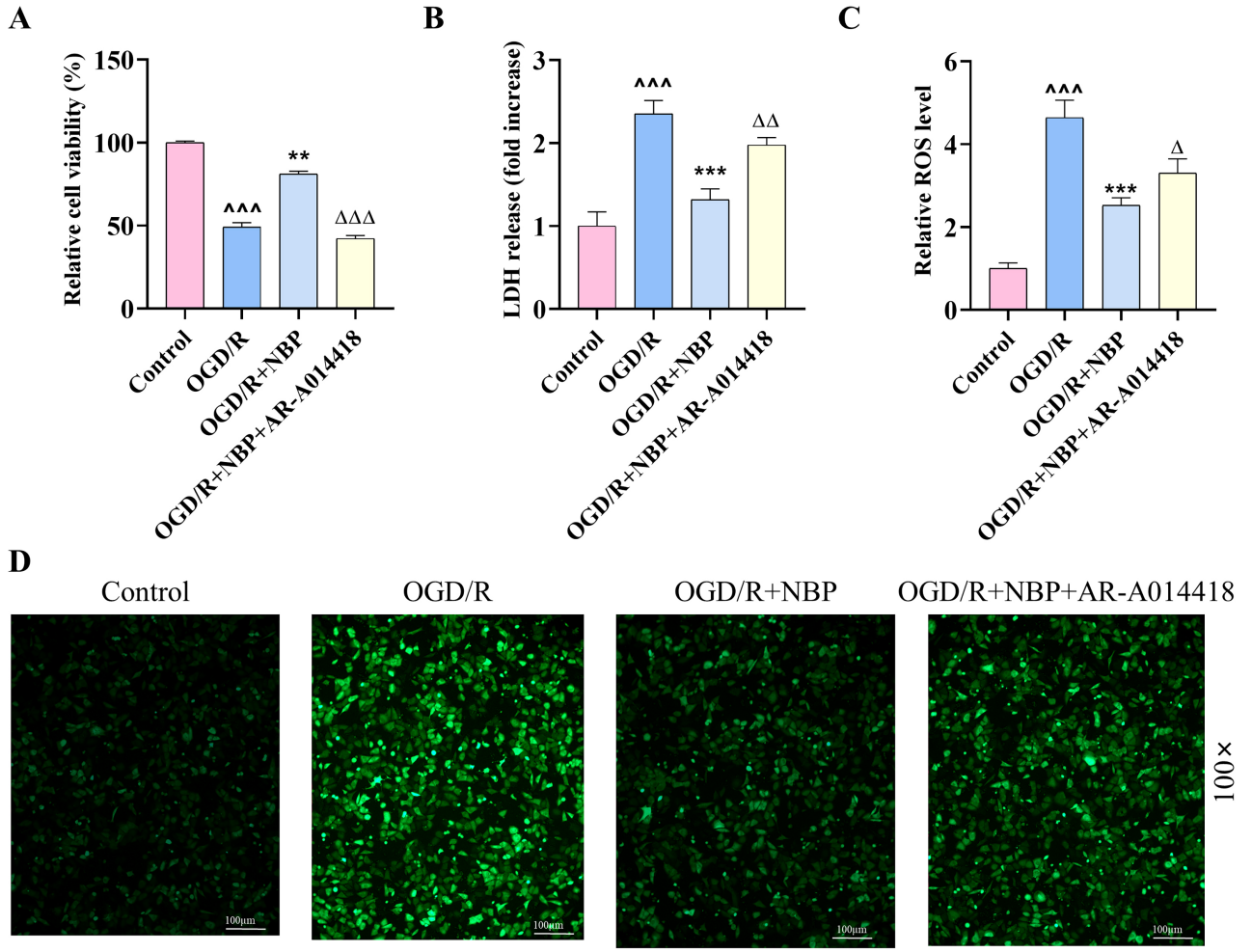


**Fig. 3. GSK-3$\beta$/NRF2 inhibitors reversed the effects of NBP on cell viability, LDH level and ROS level.** (A) Cell viability was measured using CCK8. (B) Detection of LDH levels in each group. (C,D) Dichlorodihydrofluorescein diacetate (DCFH-DA) was used to measure intracellular ROS levels. Scale: 100 μm, magnification: 100×. All datasets were derived from three independently repeated experiments. $^{\wedge}$vs. Control, $^{\wedge\wedge\wedge}p < 0.001$; $^{*}$vs. OGD/R, $^{**}p < 0.01$, $^{***}p < 0.001$; $^{\Delta}$vs. OGD/R+NBP, $^{\Delta}p < 0.05$, $^{\Delta\Delta}p < 0.01$, $^{\Delta\Delta\Delta}p < 0.001$.

## Discussion

NBP has been studied for its significant neuroprotective effects [19], including the reconstruction of microcirculation, protection of mitochondrial function, inhibition of oxidative stress, inflammatory response and neuronal apoptosis [20]. Besides, NBP is increasingly used as an adjuvant therapy for ischemic stroke [21]. Ferroptosis is an important mechanism in the occurrence of ischemic stroke. A study has found that NBP exerts protective effects on neurons from ferroptosis by activating NRF2 [16]. Our study further elucidated the detailed mechanism of NBP to improve ischemic stroke, and confirmed that NBP suppressed OGD/R-induced neuronal ferroptosis by regulating the GSK-3$\beta$/NRF2 pathway.

Ferroptosis is a distinct type of cell death characterized by intracellular iron accumulation and marked by decreased expression of GPX4 and SLC7A11 proteins. After ischemic stroke, oxidative stress is initiated, which aggravates the severity of ischemic injury [22]. Excess iron enters the brain parenchyma through a disrupted blood-brain barrier, promoting the production and accumulation of ROS, resulting in the destruction of cell structure, the leakage of nucleic acids and other intracellular substances, and ultimately inducing ferroptosis [23]. During ferroptosis, the activities of GPX4 and SOD are diminished, GSH is remarkably depleted, $Fe^{2+}$-mediated lipid peroxidation occurs, and metabolites (e.g., MDA and 4-HNE) as well as reactive free radicals (e.g., ROS, reactive nitrogen species (RNS), and reactive lipid species (RLS)) accumulate [24]. GPX4 can inhibit the levels of lipid peroxidation and ferroptosis in ischemic and hemorrhagic stroke, and reduce the degree of brain injury after stroke. The cystine/glutamate transporter system, composed of SLC3A2 and SLC7A11, plays an important role in regulating ferroptosis, and its in-

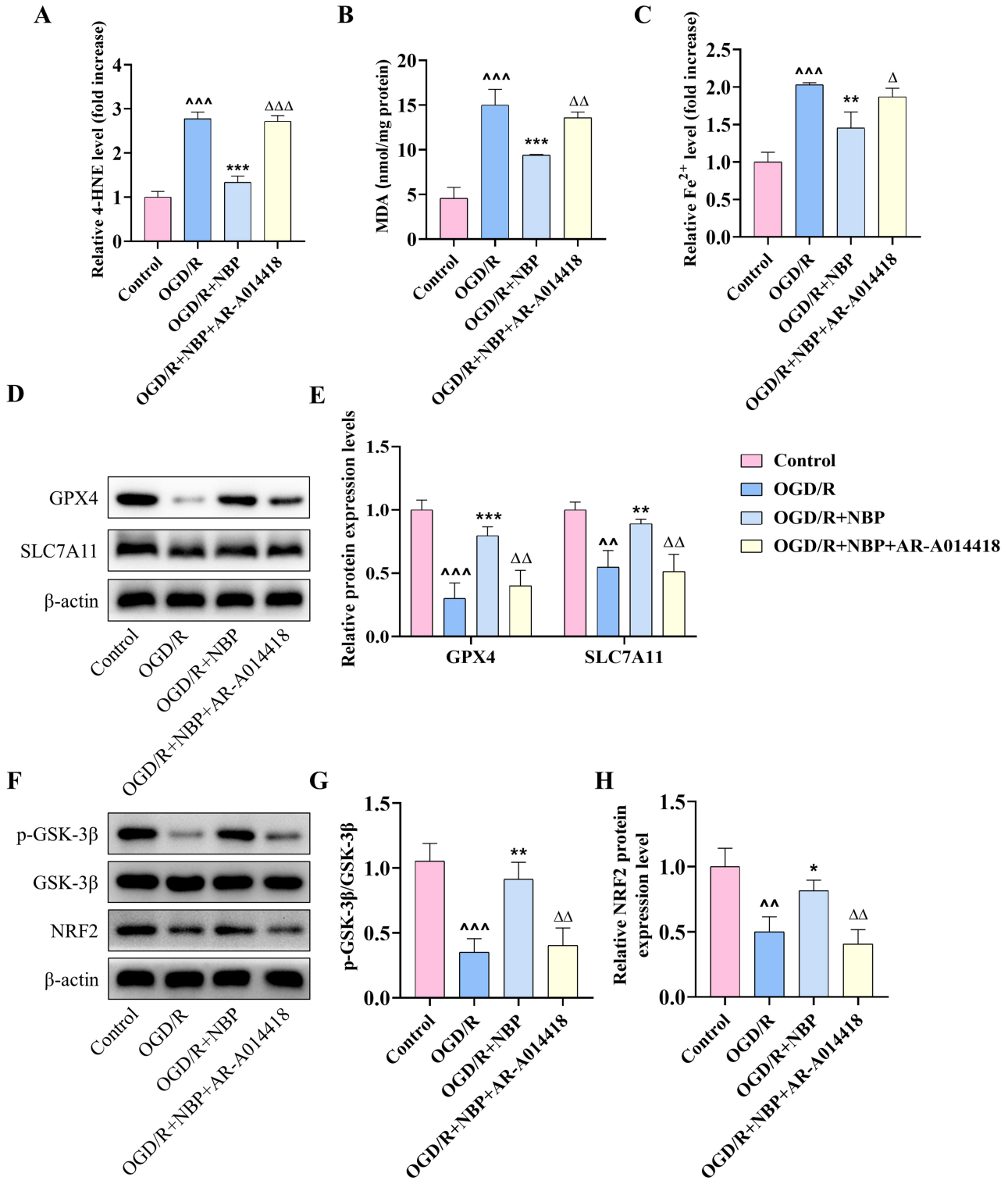


**Fig. 4. GSK-3$\beta$/NRF2 inhibitors reversed the effects of NBP on OGD/R-induced neuronal ferroptosis.** (A,B) ELISA was used to detect 4-HNE and MDA levels. (C) Detection of intracellular $Fe^{2+}$ content. (D,E) Western blot analysis of ferroptosis-related proteins GPX4 (17 kDa) and SLC7A11 (55 kDa). $\beta$-actin (42 kDa) was the internal reference. (F–H) Western blot analysis of GSK-3$\beta$ (47 kDa) phosphorylation and NRF2 (97 kDa) protein levels. $\beta$-actin (42 kDa) was the internal reference. All datasets were derived from three independently repeated experiments. $^{\wedge}$vs. Control, $^{\wedge\wedge}p < 0.01$, $^{\wedge\wedge\wedge}p < 0.001$; $^{*}$vs. OGD/R, $^{*}p < 0.05$, $^{**}p < 0.01$, $^{***}p < 0.001$; $^{\Delta}$vs. OGD/R+NBP, $^{\Delta}p < 0.05$, $^{\Delta\Delta}p < 0.01$, $^{\Delta\Delta\Delta}p < 0.001$.

hibition restricts cystine uptake, thereby blocking the synthesis of GSH, decreasing the cellular antioxidant capacity, and ultimately inducing ferroptosis [25]. A study has proven that inhibition of SLC7A11 expression can reduce GSH level and GPX4 activity, resulting in accumulation of lethal lipid peroxides, imbalance of cellular oxidative stress level, and induction of ferroptosis [18]. The results of this study suggested that OGD/R induced oxidative stress and ferroptosis in primary neuronal cells, which was reversed by NBP intervention, as evidenced by up-regulation of GPX4 and SLC7A11 proteins.

GSK-3$\beta$ is a serine/threonine protein kinase involved in a variety of cellular processes and diseases, including cell proliferation, DNA repair, cell cycle, signaling and metabolic pathways, diabetes, cancer, and Alzheimer's disease [26]. Studies have shown that GSK-3$\beta$ plays a key role in regulating and degrading NRF2, and that GSK-3$\beta$, when activated, protects cells from inflammation and oxidative damage by mediating NRF2 [27]. NRF2 is a nuclear transcription factor, and activation of the NRF2 pathway constitutes a key therapeutic approach for neurodegenerative disorders involving oxidative stress and neuroinflammation. NRF2 is activated by ROS, while persistent ROS production leads to brain damage and dysfunction [28,29]. The activation of GSK-3$\beta$ effectively protects against neuronal damage caused by Alzheimer's disease [30]. Therefore, the GSK-3$\beta$/NRF2 signaling pathway may be one of the important mechanisms of neuronal ferroptosis. Correspondingly, in our study, based on OGD/R-induced cells receiving GSK-3$\beta$ inhibitor AR-A014418 and/or NBP treatment, we found that NBP could activate GSK-3$\beta$/NRF2 pathway to suppress OGD/R-induced neuronal ferroptosis, which was specifically manifested as suppression of cellular oxidative stress, promotion of GSK-3$\beta$ phosphorylation and up-regulation of NRF2 protein levels, thereby alleviating ischemic stroke.

This study is limited to *in vitro* experiments, and further animal and clinical studies are needed. The OGD/R model used in this study cannot fully replicate the complex *in vivo* microenvironment of ischemic stroke, such as glial cell interactions, the blood-brain barrier, and systemic inflammation. Future research should validate these findings in animal experiments to explore whether NBP exerts its protective effects via the same pathway *in vivo*, thereby providing a robust reference for its clinical utility.

## Conclusion

In summary, our study demonstrates that NBP exerts a protective effect on brain injury in high-risk ischemic stroke. NBP treatment can promote OGD/R-induced primary neuronal cell activity, inhibit oxidative stress, and elevate GPX4 and SLC7A11 protein levels. These protective effects are mechanistically linked to the inhibition of OGD/R-induced neuronal ferroptosis via regulation of the GSK-3$\beta$/NRF2 pathway.

## Availability of Data and Materials

The datasets used and/or analyzed during the current study are available from the corresponding author upon reasonable request.

## Author Contributions

YC: Conceptualization, Data curation, Formal analysis, Funding acquisition, Writing—original draft, Writing—review & editing. YZ: Data curation, Formal analysis, Methodology, Writing—original draft, Writing—review & editing. JW: Data curation, Validation, Methodology, Writing—original draft, Writing—review & editing. LZ: Validation, Visualization, Formal analysis, Writing—original draft, Writing—review & editing. YH: Software, Methodology, Data curation, Writing—original draft, Writing—review & editing. HL: Validation, Methodology, Supervision, Writing—original draft, Writing—review & editing. SJ: Data curation, Visualization, Investigation, Writing—original draft, Writing—review & editing. JY: Supervision, Formal analysis, Investigation, Writing—original draft, Writing—review & editing. SL: Visualization, Project administration, Resources, Writing—original draft, Writing—review & editing. ZL: Methodology, Validation, Software, Writing—original draft, Writing—review & editing. All authors gave final approval of the version to be published. All authors have participated sufficiently in the work to take public responsibility for appropriate portions of the content and agreed to be accountable for all aspects of the work in ensuring that questions related to its accuracy or integrity.

## Ethics Approval and Consent to Participate

Not applicable.

## Acknowledgment

Not applicable.

## Funding

This work was supported by the Central Guidance for Local Science and Technology Development Funding Project (Basic Research on Free Exploration) [grant number: 246Z7732G].

## Conflict of Interest

The authors declare no conflict of interest.

## References

[1] Feigin VL, Nguyen G, Cercy K, Johnson CO, Alam T, Parmar PG, *et al*. Global, Regional, and Country-Specific Lifetime Risks of Stroke, 1990 and 2016. The New England Journal of

Medicine. 2018; 379: 2429–2437. https://doi.org/10.1056/NEJMoa1804492.

[2] Zhao Y, Zhang X, Chen X, Wei Y. Neuronal injuries in cerebral infarction and ischemic stroke: From mechanisms to treatment (Review). International Journal of Molecular Medicine. 2022; 49: 15. https://doi.org/10.3892/ijmm.2021.5070.

[3] Fang J, Wang Z, Miao CY. Angiogenesis after ischemic stroke. Acta Pharmacologica Sinica. 2023; 44: 1305–1321. https://doi.org/10.1038/s41401-023-01061-2.

[4] Zhi M, Hu L, Geng F, Shao N, Liu Y. Analysis of the Cost and Case-mix of Post-acute Stroke Patients in China Using Quantile Regression and the Decision-tree Models. Risk Management and Healthcare Policy. 2022; 15: 1113–1127. https://doi.org/10.2147/RMHP.S361385.

[5] Hankey GJ. Stroke. Lancet. 2017; 389: 641–654. https://doi.org/10.1016/S0140-6736(16)30962-X.

[6] Kuriakose D, Xiao Z. Pathophysiology and Treatment of Stroke: Present Status and Future Perspectives. International Journal of Molecular Sciences. 2020; 21: 7609. https://doi.org/10.3390/ijms21207609.

[7] Dong Y, Yin J, Chen T, Wen J, Zhang Q, Li X, *et al*. Dl-3-n-butylphthalide pretreatment attenuates renal ischemia/reperfusion injury. Biochemical and Biophysical Research Communications. 2021; 557: 166–173. https://doi.org/10.1016/j.bbrc.2021.04.006.

[8] Zhang X, Wu Q, Wang Z, Li H, Dai J. Keap1-Nrf2/ARE signal pathway activated by butylphthalide in the treatment of ischemic stroke. American Journal of Translational Research. 2022; 14: 2637–2646.

[9] Liu Z, Wang H, Shi X, Li L, Zhou M, Ding H, *et al*. DL-3-n-Butylphthalide (NBP) Provides Neuroprotection in the Mice Models After Traumatic Brain Injury via Nrf2-ARE Signaling Pathway. Neurochemical Research. 2017; 42: 1375–1386. https://doi.org/10.1007/s11064-017-2186-z.

[10] Ye ZY, Xing HY, Wang B, Liu M, Lv PY. DL-3-n-butylphthalide protects the blood-brain barrier against ischemia/hypoxia injury via upregulation of tight junction proteins. Chinese Medical Journal. 2019; 132: 1344–1353. https://doi.org/10.1097/CM9.0000000000000232.

[11] Yang Y, Li Y, Zhang S, Cao L, Zhang Y, Fang B. miR-199a-5p from bone marrow mesenchymal stem cell exosomes promotes the proliferation of neural stem cells by targeting GSK-3$\beta$. Acta Biochimica et Biophysica Sinica. 2023; 55: 783–794. https://doi.org/10.3724/abbs.2023024.

[12] Duan J, Cui J, Yang Z, Guo C, Cao J, Xi M, *et al*. Neuroprotective effect of Apelin 13 on ischemic stroke by activating AMPK/GSK-3$\beta$/Nrf2 signaling. Journal of Neuroinflammation. 2019; 16: 24. https://doi.org/10.1186/s12974-019-1406-7.

[13] Sakata H, Niizuma K, Yoshioka H, Kim GS, Jung JE, Katsu M, *et al*. Minocycline-preconditioned neural stem cells enhance neuroprotection after ischemic stroke in rats. The Journal of Neuroscience. 2012; 32: 3462–3473. https://doi.org/10.1523/JNEUROSCI.5686-11.2012.

[14] Yu J, Yang H, Fang B, Zhang Z, Wang Y, Dai Y. mfat-1 transgene protects cultured adult neural stem cells against cobalt chloride-mediated hypoxic injury by activating Nrf2/ARE pathways. Journal of Neuroscience Research. 2018; 96: 87–102. https://doi.org/10.1002/jnr.24096.

[15] Deng X, Chu W, Zhang H, Peng Y. Nrf2 and Ferroptosis: A New Research Direction for Ischemic Stroke. Cellular and Molecular Neurobiology. 2023; 43: 3885–3896. https://doi.org/10.1007/s10571-023-01411-y.

[16] Ye Z, Li C, Liu S, Liang H, Feng J, Lin D, *et al*. Dl-3-n-butylphthalide activates Nrf2, inhibits ferritinophagy, and protects MES23.5 dopaminergic neurons from ferroptosis. Chemico-Biological Interactions. 2023; 382: 110604. https://doi.org/10.1016/j.cbi.2023.110604.

[17] Xie H, Lin Y, Fang F. AR-A014418, a glycogen synthase kinase-3$\beta$ inhibitor, mitigates lipopolysaccharide-induced inflammation in rat dental pulp stem cells via NLR family pyrin domain containing 3 inflammasome impairment. Journal of Dental Sciences. 2023; 18: 1534–1543. https://doi.org/10.1016/j.jds.2023.03.010.

[18] Yuan Y, Zhai Y, Chen J, Xu X, Wang H. Kaempferol Ameliorates Oxygen-Glucose Deprivation/Reoxygenation-Induced Neuronal Ferroptosis by Activating Nrf2/SLC7A11/GPX4 Axis. Biomolecules. 2021; 11: 923. https://doi.org/10.3390/biom11070923.

[19] Wang H, Ye K, Li D, Liu Y, Wang D. DL-3-n-butylphthalide for acute ischemic stroke: An updated systematic review and meta-analysis of randomized controlled trials. Frontiers in Pharmacology. 2022; 13: 963118. https://doi.org/10.3389/fphar.2022.963118.

[20] Xiang H, Zhang Q, Han Y, Yang L, Zhang Y, Liu Q, *et al*. Novel brain-targeting 3-n-butylphthalide prodrugs for ischemic stroke treatment. Journal of Controlled Release. 2021; 335: 498–514. https://doi.org/10.1016/j.jconrel.2021.05.045.

[21] Ding Y, Gu Z, Zhai T, Wang W, Zhang Y, Wei C, *et al*. Effect of butylphthalide on new cerebral microbleeds in patients with acute ischemic stroke. Medicine. 2020; 99: e21594. https://doi.org/10.1097/MD.0000000000021594.

[22] Guo J, Tuo QZ, Lei P. Iron, ferroptosis, and ischemic stroke. Journal of Neurochemistry. 2023; 165: 487–520. https://doi.org/10.1111/jnc.15807.

[23] Liu J, Guo ZN, Yan XL, Huang S, Ren JX, Luo Y, *et al*. Crosstalk Between Autophagy and Ferroptosis and Its Putative Role in Ischemic Stroke. Frontiers in Cellular Neuroscience. 2020; 14: 577403. https://doi.org/10.3389/fncel.2020.577403.

[24] Liu P, Feng Y, Li H, Chen X, Wang G, Xu S, *et al*. Ferrostatin-1 alleviates lipopolysaccharide-induced acute lung injury via inhibiting ferroptosis. Cellular & Molecular Biology Letters. 2020; 25: 10. https://doi.org/10.1186/s11658-020-00205-0.

[25] Koppula P, Zhuang L, Gan B. Cystine transporter SLC7A11/xCT in cancer: ferroptosis, nutrient dependency, and cancer therapy. Protein & Cell. 2021; 12: 599–620. https://doi.org/10.1007/s13238-020-00789-5.

[26] Lin J, Song T, Li C, Mao W. GSK-3$\beta$ in DNA repair, apoptosis, and resistance of chemotherapy, radiotherapy of cancer. Biochimica et Biophysica Acta. Molecular Cell Research. 2020; 1867: 118659. https://doi.org/10.1016/j.bbamcr.2020.118659.

[27] Li Y, Huang J, Wang J, Xia S, Ran H, Gao L, *et al*. Human umbilical cord-derived mesenchymal stem cell transplantation supplemented with curcumin improves the outcomes of ischemic stroke via AKT/GSK-3$\beta$/$\beta$-TrCP/Nrf2 axis. Journal of Neuroinflammation. 2023; 20: 49. https://doi.org/10.1186/s12974-023-02738-5.

[28] Teleanu DM, Niculescu AG, Lungu II, Radu CI, Vladâcenco O, Roza E, *et al*. An Overview of Oxidative Stress, Neuroinflammation, and Neurodegenerative Diseases. International Journal of Molecular Sciences. 2022; 23: 5938. https://doi.org/10.3390/ijms23115938.

[29] He F, Ru X, Wen T. NRF2, a Transcription Factor for Stress Response and Beyond. International Journal of Molecular Sciences. 2020; 21: 4777. https://doi.org/10.3390/ijms21134777.

[30] Fão L, Mota SI, Rego AC. Shaping the Nrf2-ARE-related pathways in Alzheimer's and Parkinson's diseases. Ageing Research Reviews. 2019; 54: 100942. https://doi.org/10.1016/j.arr.2019.100942.